Influence of Thermal Activation of Titania on Photoreactivity of Pt/TiO_2 in Hydrogen Production

Anna Yu. Kurenkova[1] · Anna M. Kremneva[1] · Andrey A. Saraev[1] · Vadim Murzin[2] · Ekaterina A. Kozlova[1] · Vasily V. Kaichev[1,*]

[1] Boreskov Institute of Catalysis, 630090 Novosibirsk, Russia

[2] Deutsches Elektronen-Synchrotron DESY, 22603 Hamburg, Germany

*Corresponding author. E-mail address: vvk@catalysis.ru (V.V. Kaichev)

Abstract

A series of Pt/TiO_2 photocatalysts was prepared by impregnation of fresh and thermal-activated titania (commercial Evonik Aeroxide P25 TiO_2) with an aqueous solution of H_2PtCl_6 followed by reduction in an aqueous solution of $NaBH_4$. The thermal activation was performed by annealing in air. The photocatalytic activity of the Pt/TiO_2 catalysts was measured for the hydrogen production from a mixture of glycerol under UV radiation. It was found that the activation at 300-600 °C provides an increase in the photoreactivity of resulting Pt/TiO_2 photocatalysts in the production of hydrogen while its structural and textural properties do not change. This effect is due to formation of cationic vacancies that limits fast electron-hole recombination.

Keywords photocatalysis · XPS · NEXAFS · XRD · nanoparticles

1 Introduction

Photocatalytic production of hydrogen has been actively studied since 1972, when Fujishima and Honda discovered photocatalytic splitting of water on TiO_2 [1]. These studies have shown that hydrogen can be obtained not only by the direct splitting of water into H_2 and O_2 but also by the photocatalytic reforming of organic compounds using solar energy [2–4]. The latter process may also represent an effective way for the abatement of organic pollutants in wastewater. Although the detailed mechanism of photocatalytic reactions is not clear yet, it is commonly agreed that the primary reactions responsible for the photocatalytic effect are interfacial redox reactions of electrons and holes that are generated when the semiconductor catalyst absorbs light. As compared to other semiconductor photocatalysts, titanium dioxide has shown the most promise for practical applications because of its high photoreactivity (the photonic efficiency can achieve 10% [5]), good stability, low cost, and environmental friendliness. However, pure TiO_2 exhibits insufficient photocatalytic activity due to the fast electron-hole recombination. To overcome this drawback, the separation of the electron–hole pairs in a semiconductor should be provided. This effect can be obtained, for example, by deposition of platinum and other noble metals. Platinum nanoparticles are very effective traps for electrons due to the formation of the Schottky barrier at the metal–

semiconductor contact, thereby increasing the lifetime of electron-hole pairs [6]. As a result, the addition of even 1 wt% Pt leads to an increase in the photocatalytic activity by several times [7]. Another facile technique to increase the activity of TiO_2 is its thermal treatment [8, 9]. According to the literature [9], the annealing of titania may increase the rate of decomposition of methylene blue by approximately four times.

Despite the simplicity of the latter approach, the reasons for the observed increase in activity are still under debate. Moreover, conflicting points of view are given in the literature. For example, S. Sugapriya et al. [8] studied the effect of annealing of TiO_2 nanoparticles and found that their photocatalytic performance is improved due to the transformation of amorphous titanium dioxide to anatase at 450 °C. M. Fassier et al. [9] concluded that the crystallite size is the most important controlling factor for photocatalytic activity rather than the powder specific surface area or the anatase/rutile polymorph ratio. In contrast, R. Su et al. [10] found strong influence of the anatase/rutile ratio on the photoreactivity in the oxidation of methylene blue under UV radiation.

Herein we present a new insight into the thermal activation of TiO_2-based photocatalysts. To elucidate the origin of this effect we prepared Pt/TiO_2 photocatalysts using fresh and thermal-activated Evonik Aeroxide P25 TiO_2 and checked their photoreactivity in the hydrogen production. We chose the photocatalytic production of hydrogen from an aqueous solution of glycerol as a case photocatalytic reaction due to its practical importance. Indeed, glycerol is one of biomass-derived materials, and it is produced in large amounts as a by-product in the transesterification of vegetable oils into biodiesel fuels [4]. Besides, photoreforming of glycerol can provide the yield of seven moles of hydrogen from one mole of glycerol under mild conditions that is made this process suitable for industrial applications.

2 Experimental

2.1 Materials

To prepare the photocatalysts, we used commercial Evonik Aeroxide P25 (formerly known as Degussa P25) titanium dioxide synthesized via flame pyrolysis of $TiCl_4$. Fresh Aeroxide consists of multiphase TiO_2 nanoparticles containing anatase, rutile, and a small amount of amorphous TiO_2 [11]. The thermal activation of titania was performed by calcination in air at 300, 400, 500, 600, 700, or 800 °C in a programmable electric furnace. This heat treatment was performed for approximately 5 h; the thermal profile included the slow heating from room temperature to the desired temperature during 1 h with a constant heating rate, the temperature holding with an accuracy of 10 °C for 3 h, and the spontaneous cooling after turning off the furnace. The Pt/TiO_2 photocatalysts were prepared by impregnation of fresh or calcinated titania with an aqueous solution of H_2PtCl_6 (Reakhim, Russia, 98%) followed by reduction in an aqueous solution of

$NaBH_4$ (Acros Organics, 98%) at room temperature [7]. The photocatalysts were referred to as "T300", "T400", "T500", "T600", "T700", and "T800", respectively. The photocatalyst prepared without the thermal activation was referred to as "RT". Platinum content was approximately 1 wt% in all the photocatalysts. All the chemical reagents used in the experiments, excluding distilled water, were obtained from commercial sources as guaranteed-grade reagents and were used without further purification and treatment.

2.2 Methods

The photocatalysts were examined by UV-vis spectroscopy, X-ray photoelectron spectroscopy (XPS), X-ray absorption near edge structure (XANES) spectroscopy, and X-ray diffraction (XRD) and N_2 adsorption techniques. The diffuse reflectance UV-vis spectra were obtained using a Shimadzu UV-2501 PC spectrophotometer with an ISR-240A diffuse reflectance unit. The specific surface area (SSA) was calculated by the Brunauer–Emmett–Teller method using nitrogen adsorption isotherms measured at liquid nitrogen temperatures with an automatic Micromeritics ASAP 2400 sorptometer. XRD patterns were recorded on a Bruker D8 Advance diffractometer in the 2θ range from 20° to 80° using the Cu *Kα* radiation. The mean sizes of crystallites in the samples were estimated from the full width at half maximum of corresponding peaks using the Scherrer formula. The phase composition of the photocatalysts was quantitatively analyzed using the Rietveld refinement method.

The XPS study was performed using an X-ray photoelectron spectrometer (SPECS Surface Nano Analysis GmbH, Germany) equipped with a PHOIBOS-150 hemispherical electron energy analyzer, a XR-50M X-ray source, and an ellipsoidal crystal monochromator FOCUS-500. The core-level spectra were obtained under ultrahigh vacuum conditions using the monochromatic Al *Kα* radiation. The charge correction was performed by setting the Ti$2p_{3/2}$ peak at 459.0 eV [12]. In this case, the main peak in the C*1s* spectra was observed at 285.2±0.1 eV. Relative concentrations of elements were determined from the integral intensities of the core-level spectra using the cross sections according to Scofield [13]. For detailed analysis, the spectra were fitted into several peaks after the background subtraction by the Shirley method. The fitting procedure was performed using the CasaXPS software. The line shapes of the peaks were approximated by the multiplication of Gaussian and Lorentzian functions.

The Ti K-edge XANES spectra of the Pt/TiO_2 photocatalysts and reference anatase and rutile samples were obtained at the P65 beamline at the synchrotron radiation facility PETRA III (DESY, Hamburg) [14]. A double-crystal fixed-exit monochromator based on Si(111) single-crystals designed by Oxford Ltd. was used. The monochromator was cooled to liquid nitrogen temperature in order to reduce lattice strain by the heat-load impinging on the first crystal. XANES spectra were

measured in the fluorescence detection mode using a passivated implanted planar silicon (PIPS) detector. The XANES spectra were analyzed with the Demeter (IFEFFIT) program package [15].

The photocatalytic activity of the Pt/TiO_2 catalysts was measured for the hydrogen production from a mixture of glycerol and water in a laboratory-made batch reactor. The experiments were performed at atmospheric pressure and at room temperature. The volume of the reactor was 125 cm^3. Before the experiment, 50 mg of a photocatalyst was suspended in the solution, which contained 2.8 mL of glycerol, 97.2 mL of water, and 200 mg of NaOH. The reactor was loaded by this suspension and then was purged with Ar for 30 min. After that, the suspension was illuminated using a 30 W LED lamp with a wavelength of 380 nm (the emission spectrum is present in Fig. S1). The procedure for determining the rate of hydrogen production is described in detail in Supporting Information.

3 Results and discussion

Aeroxide is cheap and extremely photoactive in many photocatalytic reactions, and as a result has become almost the "gold standard" in semiconductor photochemistry research [16]. However, bare Aeroxide exhibits a very low activity in photoreforming of glycerol (0.15 μmol H_2 min^{-1} for the uncalcinated sample). The platinum deposition leads to an increase in activity by more than an order of magnitude. The results of photocatalytic tests of the fresh and thermal-activated platinized samples are presented in Fig. 1. One can see that the thermal treatment increases photoreactivity of Pt/TiO_2 in the hydrogen production. An exception is the sample calcined at 800 °C, which exhibits a very low activity. The maximum activity, 3.6 mmol H_2 min^{-1}, or 4.3 mmol g^{-1} h^{-1} is observed for the sample calcined at 500 °C, while the further increase of the calcination temperature leads to a decrease in the photoactivity. The highest quantum efficiency is 1.2% (λ = 380 nm). This value is quite good for the hydrogen production from a glycerol solution (Table S1).

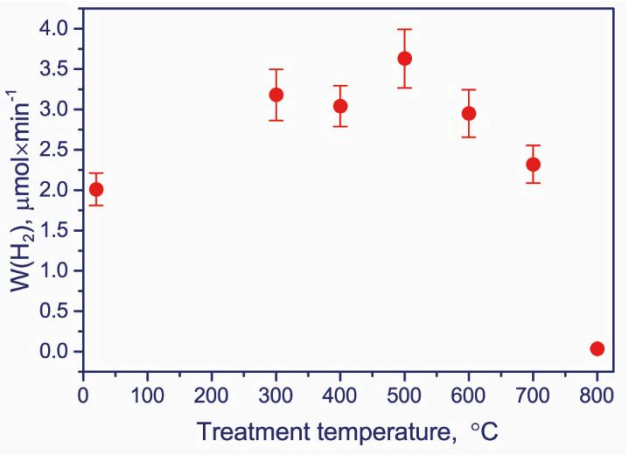

Fig. 1 Photocatalytic production of hydrogen from an aqueous solution of glycerol on Pt/TiO_2 under UV radiation depending on the calcination temperature

To refine the activation effects, morphology, chemistry, and phase composition of the photocatalysts were studied. Table 1 shows the main properties of the fresh and thermal-activated Pt/TiO_2 photocatalysts. All the samples exhibit well developed XRD patterns (Fig. S2), which match well with anatase, rutile, and metallic platinum.

No changes in the structural and textural properties were observed after the calcination at temperatures below 600 °C. According to the Rietveld refinement, the ratio of anatase to rutile (A/R) in the uncalcined photocatalysts and in the Pt/TiO_2 photocatalysts calcined at 300, 400, and 500 °C is 85/15. The mean size of crystallites (D) determined by the Scherrer formula for anatase and platinum is also constant, while the mean size of rutile crystallites increases slightly with the calcination temperature. The specific surface area and the pore volume V are 52-55 m^2/g and 0.43-0.50 cm^3/g, respectively; some deviation observed in these values is due to experimental errors. All these parameters drastically change after the calcination at 700 and 800 °C due to rutile formation. Indeed, it is well known that titanium dioxide, the only naturally occurring oxide of titanium at atmospheric pressure, exhibits three polymorphs: rutile, anatase, and brookite [17]. While rutile is the stable phase, both anatase and brookite are metastable. In the photocatalysts under study, brookite was not detected. At temperature above 600 °C, anatase starts to transform to rutile and after the calcination at 800 °C, no anatase was detected by XRD. This process is accompanied by a strong decrease in the specific surface area and in the pore volume, whereas the mean size of rutile crystallites increases from 32 to 125 nm (Table 1).

Table 1 Properties of fresh and thermal-activated Pt/TiO_2 photocatalysts

Sample	D* of anatase, nm	D* of rutile, nm	D* of Pt, nm	A/R from XRD	A/R from XANES	SSA, m^2/g	V**, cm^3/g	[O]/[Ti] from XPS TiO_2
RT	19	30	4.6	85/15	89/11	55	0.48	2.07
T300	19	30	4.4	85/15	90/10	55	0.50	2.16
T400	19	31	4.6	85/15	86/14	53	0.43	2.26
T500	19	31	4.5	85/15	85/15	52	0.49	2.42
T600	19	32	4.3	84/16	87/13	55	0.52	2.41
T700	29	74	4.4	14/86	22/78	19	0.074	2.69
T800	-	125	5.3	0/100	0/100	10	0.035	2.43

* Crystalline size calculated using the Scherrer equation

** Pore volume determined by low temperature adsorption of N_2

The XRD data are confirmed by UV-vis spectroscopy. The UV-vis diffuse reflectance spectra of the fresh and thermal-activated photocatalysts are presented in Fig. 2. All the spectra contain a single steep absorption edge around 400 nm corresponding to its bandgap. The spectra of the photocatalysts calcined at 700 and 800 °C show a red shift, indicating formation of rutile. Indeed, the optical properties of titanium dioxide depend on its crystal structure. In particular, the optical bandgap of anatase is 3.23 eV (384 nm), whereas that of rutile is 3.02 eV (410 nm) [18].

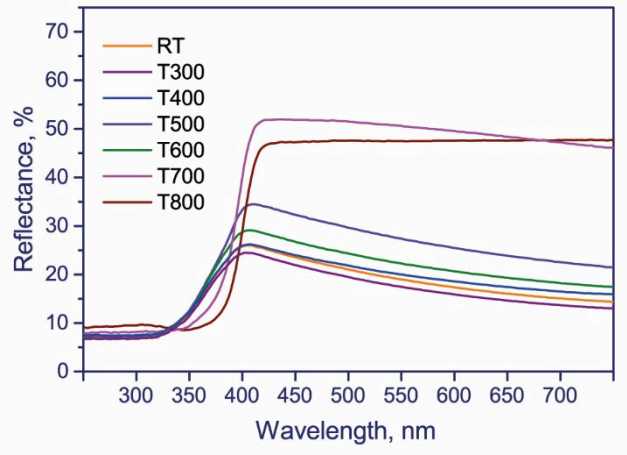

Fig. 2 Diffuse reflectance spectra of fresh and activated Pt/TiO_2 photocatalysts

Hence, our data indicate that the enhanced activity of the Pt/TiO_2 photocatalysts obtained via the thermal activation at 300-500 °C is not a result of changes in its texture properties or the anatase/rutile ratio. However, it is likely that the methods used cannot detect some structural features of the photocatalysts. For instance, R.I. Bickley et al. [19] suggested that some individual anatase nanoparticles may be covered by a thin overlayer of rutile and the photocatalytic activity of this form of titanium dioxide may be greater than the activity of either pure crystalline phase. To check the presence of an excess of rutile, undetectable by XRD, all the photocatalysts were investigated by XANES. It should be stressed that XANES are sensitive not only to the oxidation state of specific atoms but also to its local chemical environment.

The Ti K-edge XANES spectra of the Pt/TiO_2 photocatalysts are presented in Fig. 3a in comparison to the spectra of bulk anatase and bulk rutile. One can see that the spectra of anatase and rutile differ significantly. The spectrum of anatase contains two strong peaks at 4987 and 5003 eV, while the spectrum of rutile contains three strong peaks at 4987, 4992, and 5004 eV. This is in full agreement with the literature [20]. The spectra of the fresh Pt/TiO_2 photocatalyst and the Pt/TiO_2 photocatalysts calcined at 300-500 °C are similar to the spectrum of anatase, whereas the spectra of the Pt/TiO_2 photocatalysts calcined at 700 and 800 °C are similar to the spectrum of rutile.

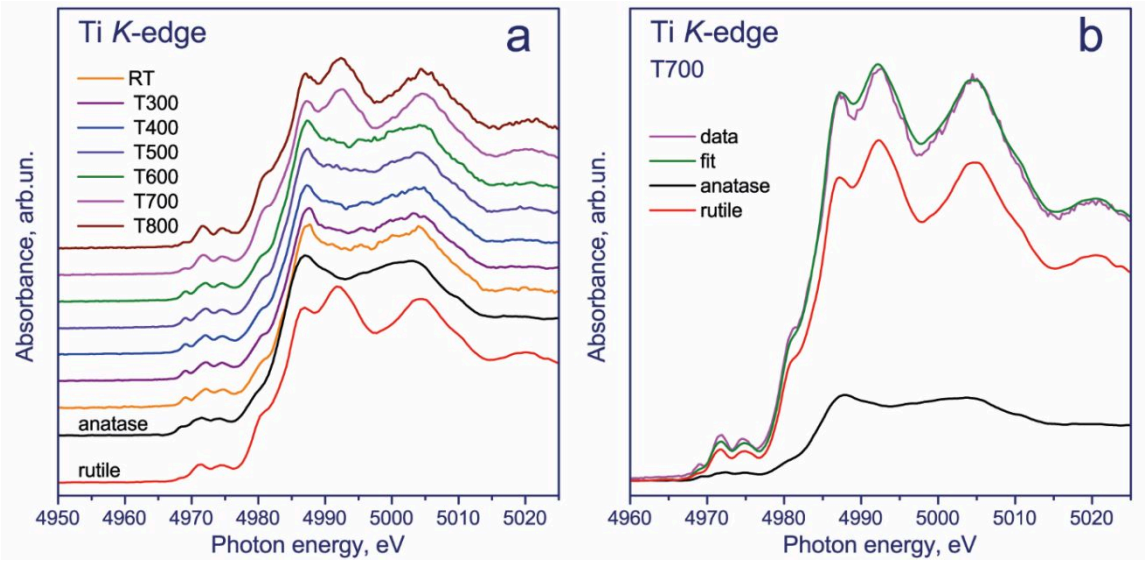

Fig. 3 Normalized Ti K-edge XANES spectra of bulk anatase, bulk rutile, and the fresh and thermally activated Pt/TiO_2 photocatalysts (a); approximation of the XANES spectrum of Pt/TiO_2-T700 by a linear combination of spectra of anatase and rutile (b)

The simplest approach in the XANES data-processing is a linear combination fitting (LCF) [21]. In the LCF method, the X-ray absorption spectrum is modelled by the least-squares fitting using a linear combination of known species to fit an unknown spectrum. In our case, the Ti K-edge XANES spectra of the photocatalysts were well approximated by a linear combination of the spectra of anatase and rutile. The approximation of the XANES spectrum of the T700 photocatalyst by a linear combination of spectra of anatase and rutile is shown in Fig. 3b.

The anatase/rutile ratios determined by the LCF method are presented in Table 1. One can see that XANES gives a higher anatase content in the photocatalysts than XRD does. We can speculate that at least the fresh photocatalyst and the samples calcined at 300 and 400 °C have this effect due to the presence of amorphous TiO_2 whose Ti K-edge XANES spectrum is similar to the spectrum of anatase [20]. The calcination at higher temperatures leads to the transformation of amorphous TiO_2 to anatase and further to rutile. As a result, both XRD and XANES give the same anatase/rutile ratio for the photocatalyst calcined at 500 °C. This finding indicated that the thermal activation at 500 °C leads to remove amorphous TiO_2 which positively affects the activity of the resulting Pt/TiO_2 photocatalyst as it provides a good contact of the platinum nanoparticles and anatase necessary for the formation of the Schottky barrier.

Finally, we investigated the photocatalysts by XPS. The Pt*4f* and Ti*2p* core-level spectra of the fresh and activated Pt/TiO_2 photocatalysts are presented in Figures 4a and 4b. It is known that the ***4f*** level of platinum splits to the Pt$4f_{7/2}$ and Pt$4f_{5/2}$ sublevels due to spin-orbital interaction. The Pt*4f* spectra of all the catalysts were approximated by one asymmetric doublet with the Pt$4f_{7/2}$ binding

energy of 71.1±0.1 eV with the spin-orbital splitting of 3.33 eV (Fig. 4a), which is typical of platinum in the metallic state [22]. For the fresh photocatalyst and the photocatalysts calcined at 300, 400, 500, and 600 °C the [Pt]/[Ti] atomic ratio is in the range 0.015-0.017, which slightly increases with the calcination temperature. The [Pt]/[Ti] atomic ratio for the Pt/TiO_2 photocatalysts calcined at 700 and 800 °C increases to 0.037 and 0.058, respectively This is in good agreement with the XRD data (Table 1), which indicates that the dispersion of the platinum nanoparticles does not change with the calcination temperature with the exception of 800 °C when the mean size of nanoparticles slightly increases because of low surface area of titania. Since XPS is a surface-sensitive method, the increase in the [Pt]/[Ti] atomic ratio for the T700 and T800 photocatalysts is caused by a decrease in the specific surface area.

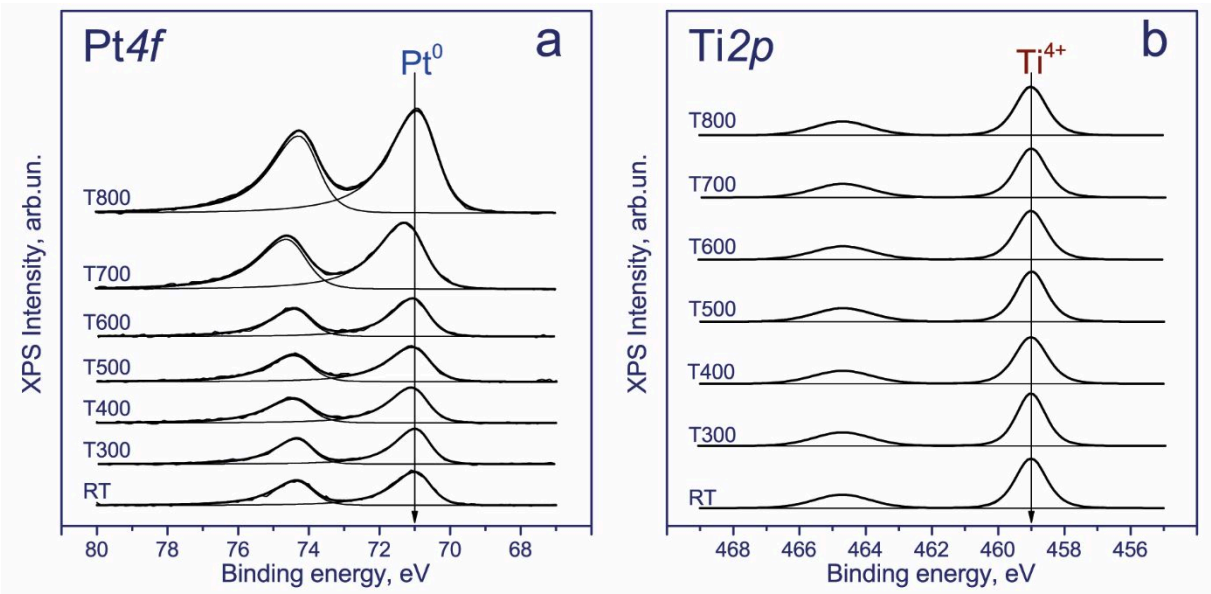

Fig. 4 Normalized Pt*4f* (a) and Ti*2p* (b) core-level spectra of studied catalysts. The Pt*4f* spectra are normalized to the integrated intensity of corresponding Ti*2p* spectra

All the Ti*2p* spectra contain two sharp peaks corresponding to the Ti$2p_{3/2}$ and Ti$2p_{1/2}$ sublevels (Fig. 4b). The peaks have symmetric shape, which is typical of titanium in the oxidized state. Taking into account the Ti$2p_{3/2}$ binding energy of 459.0 eV and the spin-orbital splitting of 5.66 eV, we concluded that titanium is mainly in the Ti^{4+} state. No additional peaks were observed at lower binding energy, which may be attributed to reduced titanium species, such as Ti^{3+}. According to the literature, the Ti$2p_{3/2}$ binding energy for TiO_2 is in the range of 458.7-459.2 eV, whereas for titanium in the Ti^{3+} state, the binding energy is between 456.2 and 457.4 eV [12]. This is an expected result because the thermal activation was performed in air. The formation of Ti^{3+} defects in TiO_2, which is usually accompanied by the formation of oxygen vacancies, was detected after the annealing of anatase in a reducing atmosphere, such as vacuum or hydrogen [23]. At the same time, we found that the calcination of TiO_2 leads to an increase in the [O]/[Ti] atomic ratio (Table 1). The

fresh Pt/TiO_2 photocatalyst is characterized by the [O]/[Ti] atomic ratio equal to 2.07, which is close to the stoichiometric value. This ratio monotonously increases from 2.16 to 2.42 when the calcination temperature increases from 300 to 500 °C. This means that the thermal activation leads to the formation of cationic vacancies.

It should be noted that the formation of cationic vacancies in titania is not a new effect. Recently, Ghosh and Nambissan [24] studied the annealing of anatase nanoparticles. Using photoluminescence spectroscopy, they showed the formation of vacancy-type defects such as oxygen vacancy (V_O), cation vacancy (V_{Ti}) or vacancy-combination defects. The application of positron annihilation spectroscopy and Coincident Doppler broadening spectroscopy made it possible to prove the formation of cation vacancy V_{Ti} and larger vacancy-combination defects as divacancy V_{Ti+O} and trivacancy $V_{Ti+O+Ti}$. During the annealing, the concentration of such defect-combinations initially increases to a maximum at approximately 300 °C and then decreases at higher temperatures due to gradual annealing. We can speculate that the divacancy V_{Ti+O} and trivacancy $V_{Ti+O+Ti}$ are also formed during the thermal activation of our photocatalysts. According to XPS (Table 1) the concentration of cation vacancies in our titania samples increases with the calcination temperature excepting 800 °C when anatase transforms to rutile in full. Being negatively charged, these defects within TiO_2 nanoparticles could play the role of hole traps, thereby increasing the lifetime of electron-hole pairs in the semiconductor and increasing their photoreactivity. Certainly, some additional experiments and DFT calculations should be performed to study in detail the formation of the cationic vacancies in titania and their role in photocatalytic reactions.

4 Conclusions

The Pt/TiO_2 photocatalysts prepared by fresh and thermal-activated Evonik Aeroxide P25 TiO_2 were tested in the production of hydrogen from aqueous solutions of glycerol under UV radiation. It was found that the thermal activation of titania in the temperature range between 300 and 600 °C leads to an increase in the photoreactivity of resulting Pt/TiO_2 photocatalysts. The highest activity was obtained after annealing at 500 °C. According to the XPS study this effect is due to formation of cationic vacancies that limit the fast electron-hole recombination. After annealing at 700-800 °C, anatase transforms irreversibly to rutile which typically has less photoreactivity due to shorter lifetime of electron-hole pairs. Moreover, the rutile formation is accompanied by a strong decrease in the specific surface area, which also negatively affects the rate of hydrogen production. Hence, the thermal activation of titania at 500 °C can be used to improve the activity of titania-based photocatalysts. In addition it was found that the thermal activation at 500 °C leads to remove amorphous TiO_2 which positively affects the activity of the resulting Pt/TiO_2 photocatalyst as it

provides a good contact of the platinum nanoparticles and anatase necessary for the formation of the Schottky barrier. Hence, both these effects, the creation of cationic vacancies and transformation of amorphous TiO_2 to anatase under the thermal activation can provide enhanced photocatalytic activity of Pt/TiO_2 photocatalysts.

Acknowledgments This work was supported by Russian Science Foundation (grant #19-73-20020). The XPS and XRD experiments were performed using facilities of the shared research center "National center of investigation of catalysts" at Boreskov Institute of Catalysis. The authors are grateful to S. Cherepanova for the XRD study and T. Larina for the UV-vis measurements. The authors are also grateful to the staff of DESY for their support during the beam time.

Compliance with Ethical Standards

Conflict of interest The authors declare that they have no conflict of interest.

Electronic supplementary material The online version of this article (https://doi.org/) contains supplementary material, which is available to authorized users.

References

1. Fujishima A, Honda K (1972) Electrochemical photolysis of water at a semiconductor electrode. Nature 238:37–38. https://doi.org/10.1038/238037a0
2. Kozlova EA, Markovskaya DV, Cherepanova SV, Saraev AA, Gerasimov EY. Perevalov TV, Kaichev VV, Parmon VN (2014) Novel photocatalysts based on $Cd_{1-x}Zn_xS/Zn(OH)_2$ for the hydrogen evolution from water solutions of ethanol. Int. J. Hydrogen Energy 39:18758–18769. https://doi.org/10.1016/j.ijhydene.2014.08.145
3. Kozlova EA, Parmon VN (2017) Heterogeneous semiconductor photocatalysts for hydrogen production from aqueous solutions of electron donors. Russ Chem Rev 86:870–906. https://doi.org/10.1070/RCR4739
4. Fujita SI, Kawamori H, Honda D, Yoshida H, Arai M (2016) Photocatalytic hydrogen production from aqueous glycerol solution using NiO/TiO_2 catalysts: Effects of preparation and reaction conditions. Appl Catal B 181:818–824. https://doi.org/10.1016/j.apcatb.2015.08.048
5. Schneider J, Matsuoka M, Takeuchi M, Zhang J, Horiuchi Y (2014) Understanding TiO_2 photocatalysis: Mechanisms and materials. Chem Rev 114:9919–9986. https://doi.org/10.1021/cr5001892
6. Linsebigler AL, Lu G, Yates JT, Jr (1995) Photocatalysis on TiO_2 surfaces: Principles, mechanisms, and selected results. Chem Rev 95:735–758. https://doi.org/10.1021/cr00035a013

7. Kozlova EA, Lyubina TP, Nasalevich MA, Vorontsov AV, Miller AV, Kaichev VV, Parmon VN (2011) Influence of the method of platinum deposition on activity and stability of Pt/TiO_2 photocatalysts in the photocatalytic oxidation of dimethyl methylphosphonate. Catal Commun 12:597–601. https://doi.org/10.1016/j.catcom.2010.12.007
8. Sugapriya S, Sriram R, Lakshmi S (2013) Effect of annealing on TiO_2 nanoparticles. Optik 124:4971–4975. https://doi.org/10.1016/j.ijleo.2013.03.040
9. Fassier M, Peyratout CS, Smith DS, Ducroquetz C, Voland T (2010) Photocatalytic activity of titanium dioxide coatings: Influence of the firing temperature of the chemical gel. J Eur Ceram Soc 30:2757–2762. https://doi.org/10.1016/j.jeurceramsoc.2010.05.018
10. Su R, Bechstein R, Sø L, Vang RT, Sillassen M, Esbjörnsson B, Palmqvist A, Besenbacher F (2011) How the anatase-to-rutile ratio influences the photoreactivity of TiO_2. J Phys Chem C 115:24287–24292. https://doi.org/10.1021/jp2086768
11. Jiang X, Manawan M, Feng T, Qian R, Zhao T, Zhou G, Kong F, Wang Q, Dai S, Pan JH (2018) Anatase and rutile in evonik aeroxide P25: Heterojunctioned or individual nanoparticles? Catal Today 300:12–17. https://doi.org/10.1016/j.cattod.2017.06.010
12. Kaichev VV, Popova GY, Chesalov YA, Saraev AA, Zemlyanov DY, Beloshapkin SA, Knop-Gericke A, Schlögl R, Andrushkevich TV, Bukhtiyarov VI (2014) Selective oxidation of methanol to form dimethoxymethane and methyl formate over a monolayer V_2O_5/TiO_2 catalyst. J Catal 311:59–70. http://doi.org/10.1016/j.jcat.2013.10.026
13. Scofield JH (1976) Hartree-Slater subshell photoionization cross-sections at 1254 and 1487 eV. J Electron Spectrosc Relat Phenom 8:129–137. https://doi.org/10.1016/0368-2048(76)80015-1
14. Caliebe WA, Murzin V, Kalinko A, Görlitz M (2019) High-flux XAFS-beamline P64 at PETRA III. AIP Conf Proc 2054:060031. https://doi.org/10.1063/1.5084662
15. Ravel B, Newville M (2005) ATHENA, ARTEMIS, HEPHAESTUS: data analysis for X-ray absorption spectroscopy using IFEFFIT. J Synchrotron Rad 12:537–541. https://doi.org/10.1107/S0909049505012719
16. Mills A, Lee SK (2002) A web-based overview of semiconductor photochemistry-based current commercial applications. J Photochem Photobiology A 152:233–247. https://doi.org/10.1016/S1010-6030(02)00243-5
17. Hanaor DAH, Sorrell CC (2011) Review of the anatase to rutile phase transformation. J Mater Sci 46:855–874. https://doi.org/10.1007/s10853-010-5113-0
18. Mills A, Lee SK (2003) Platinum group metals and their oxides in semiconductor photosensitization. Platinum Metals Rev 47:2–12. https://www.technology.matthey.com/article/47/1/2-12/

19. Bickley RI, Gonzalez-Carreno T, Lees JS, Palmisano L, Tilley RJD (1991) A structural investigation of titanium dioxide photocatalysts. J Solid State Chem 92:178–190. http://dx.doi.org/10.1016/0022-4596(91)90255-G
20. Zhang H, Chen B, Banfield JF (2008) Atomic structure of nanometer-sized amorphous TiO_2. Phys Rev B 78:214106. https://doi.org/10.1103/PhysRevB.78.214106
21. Fedorov AV, Tsapina AM, Bulavchenko OA, Saraev AA, Odegova GV, Ermakov DY, Zubavichus YV, Yakovlev VA, Kaichev VV (2018) Structure and chemistry of Cu–Fe–Al nanocomposite catalysts for CO oxidation. Catal Lett 148:3715–3722. https://doi.org/10.1007/s10562-018-2539-5
22. Miller AV, Kaichev VV, Prosvirin IP, Bukhtiyarov VI (2013) Mechanistic study of methanol decomposition and oxidation on Pt(111). J Phys Chem C 117:8189–8197. https://doi.org/10.1021/jp3122177
23. Xiong LB, Li JL, Yang B, Yu Y (2011) Ti^{3+} in the surface of titanium dioxide: Generation, properties and photocatalytic application. J Nanomater 2012:831524. https://doi.org/10.1155/2012/831524
24. Ghosh S, Nambissan PMG (2019) Evidence of oxygen and Ti vacancy induced ferromagnetism in post-annealed undoped anatase TiO_2 nanocrystals: A spectroscopic analysis. J Solid State Chem 275:174–180. https://doi.org/10.1016/j.jssc.2019.04.010

Electronic supplementary material (ESM)

Influence of Thermal Activation of Titania on Photoreactivity of Pt/TiO_2 in Hydrogen Production

Anna Yu. Kurenkova[1] · Anna M. Kremneva[1] · Andrey A. Saraev[1] · Vadim Murzin[2] · Ekaterina A. Kozlova[1] · Vasily V. Kaichev[1,*]

[1] Boreskov Institute of Catalysis, 630090 Novosibirsk, Russia

[2] Deutsches Elektronen-Synchrotron DESY, 22603 Hamburg, Germany

*Corresponding author. E-mail address: vvk@catalysis.ru (V.V. Kaichev).

The photocatalytic activity of the Pt/TiO_2 catalysts was measured for the hydrogen production from a mixture of glycerol (Vekton, analytical grade) and water in a laboratory-made batch reactor. The experiments were performed at atmospheric pressure and at room temperature. The volume of the reactor was 125 cm^3. Before the experiment, 50 mg of a photocatalyst was suspended in the solution, which contained 2.8 mL of glycerol, 97.2 mL of water, and 200 mg of NaOH (Reachim, analytical grade). The reactor was loaded by this suspension and then was purged with Ar for 30 min. After that, the suspension was illuminated using a 30 W LED with a wavelength of 380 nm (1.0 A; 71 mW/cm^2, S = 22.5 cm^2). The emission spectrum of the LED light source is presented in Fig. S1.

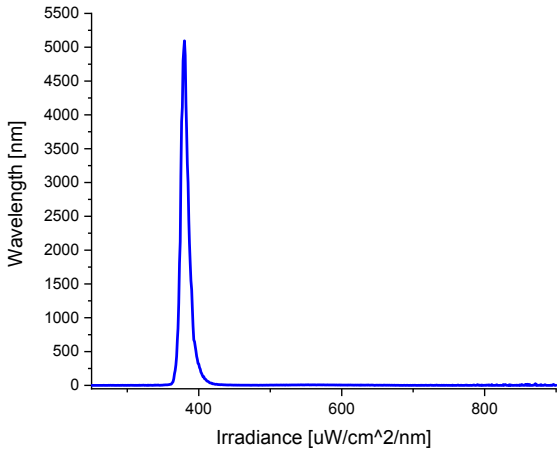

Fig. S1 Emission spectrum of used LED light source

Apparent quantum yield was calculated according to the following equation:

$$AQE = \frac{W_0(H_2)}{N_{phot}},$$

where W_0 (H_2) is the initial rate of hydrogen production in μmol/min, N_{phot} is the whole number of photons reached the sample.

N_{phot} was calculated according to the formula:

$$N \times S = N_{phot} \times h\frac{c}{\lambda},$$

where N is light intensity, S is the area of light spot, N_{phot} is the photon flux, $h\frac{c}{\lambda}$ is energy of quant of light. The calculated photon flux was equal to 310 μE/min. The power density measurements were conducted using a ThorLabs PM100USB apparatus with a ThorLabs S401C thermobaric detector. The spectrum of action of the irradiation source is controlled by a small-sized optical fiber spectrometer Ocean Optics USB4000-UV-VIS-ES. The amount of evolved H_2 was measured by a Khromos GC-1000 gas chromatograph (Khromos, Russia) equipped with a zeolite column and a thermal conductivity detector using argon as the carrier gas.

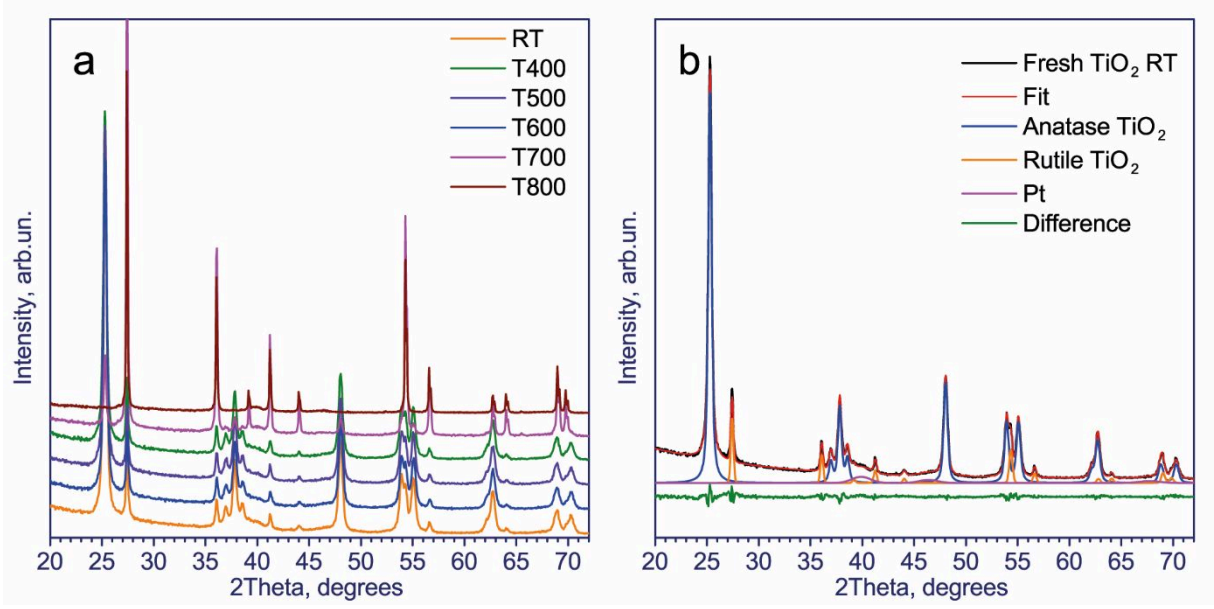

Fig. S2 XRD patterns of the fresh and activated Pt/TiO_2 photocatalysts (a); curve-fitting analysis of the XRD pattern of the fresh Pt/TiO_2 photocatalyst

Table S1 The comparison of activity for some photocatalysts in the hydrogen evolution reaction from glycerol aqueous solutions

Photocatalyst	**Special conditions**	**W, μmol·H_2 h^{-1}·g_{cat}^{-1}**	**Ref**
ZnO/ZnS–PdS	150 W high-pressure mercury lamp (365 nm), T = 80 °C	2140	1
ZnO-ZnS	300 W high-pressure mercury lamp (365 nm)	193	2
ZnO-ZnS/graphene		1070	
Cu/TiO_2	solar irradiation	16800	3
Ag/TiO_2		6370	
Co/TiO_2		1860	
Pt/TiO_2-F	365 nm	2170	4
1%Pt/TiO_2 (T = 500 ºC)	380 nm	4320	Present study

References

1. S. Liu, X. Wang, K. Wang, R. Lv, Y. Xu, Appl. Surf. Sci. 283 (2013) 732-739.
2. C.-J. Chang, Y.-G. Lin, H.-T. Weng, Y.-H. Wei, Appl. Surf. Sci. 451 (2018) 198-206.
3. T. W.P. Seadira, G. Sadanandam, T. Ntho, C. M. Masuku, M. S. Scurrell, Appl. Catal. B 222 (2018) 133-145.
4. V. Vaiano, M.A. Lara, G. Iervolino, M. Matarangolo, J.A. Navio, M.C. Hidalgo, J. Photochem. Photobiolgy A 365 (2018) 52-59.

Influence of Thermal Activation of Titania on Photoreactivity of Pt/TiO_2 in Hydrogen Production

Anna Yu. Kurenkova[1] · Anna M. Kremneva[1] · Andrey A. Saraev[1] · Vadim Murzin[2] · Ekaterina A. Kozlova[1] · Vasily V. Kaichev[1,*]

[1] Boreskov Institute of Catalysis, 630090 Novosibirsk, Russia

[2] Deutsches Elektronen-Synchrotron DESY, 22603 Hamburg, Germany

*Corresponding author. E-mail address: vvk@catalysis.ru (V.V. Kaichev)

Abstract

A series of Pt/TiO_2 photocatalysts was prepared by impregnation of fresh and thermal-activated titania (commercial Evonik Aeroxide P25 TiO_2) with an aqueous solution of H_2PtCl_6 followed by reduction in an aqueous solution of $NaBH_4$. The thermal activation was performed by annealing in air. The photocatalytic activity of the Pt/TiO_2 catalysts was measured for the hydrogen production from a mixture of glycerol under UV radiation. It was found that the activation at 300-600 °C provides an increase in the photoreactivity of resulting Pt/TiO_2 photocatalysts in the production of hydrogen while its structural and textural properties do not change. This effect is due to formation of cationic vacancies that limits fast electron-hole recombination.

Keywords photocatalysis · XPS · NEXAFS · XRD · nanoparticles

1 Introduction

Photocatalytic production of hydrogen has been actively studied since 1972, when Fujishima and Honda discovered photocatalytic splitting of water on TiO_2 [1]. These studies have shown that hydrogen can be obtained not only by the direct splitting of water into H_2 and O_2 but also by the photocatalytic reforming of organic compounds using solar energy [2–4]. The latter process may also represent an effective way for the abatement of organic pollutants in wastewater. Although the detailed mechanism of photocatalytic reactions is not clear yet, it is commonly agreed that the primary reactions responsible for the photocatalytic effect are interfacial redox reactions of electrons and holes that are generated when the semiconductor catalyst absorbs light. As compared to other semiconductor photocatalysts, titanium dioxide has shown the most promise for practical applications because of its high photoreactivity (the photonic efficiency can achieve 10% [5]), good stability, low cost, and environmental friendliness. However, pure TiO_2 exhibits insufficient photocatalytic activity due to the fast electron-hole recombination. To overcome this drawback, the separation of the electron–hole pairs in a semiconductor should be provided. This effect can be obtained, for example, by deposition of platinum and other noble metals. Platinum nanoparticles are very effective traps for electrons due to the formation of the Schottky barrier at the metal–

semiconductor contact, thereby increasing the lifetime of electron-hole pairs [6]. As a result, the addition of even 1 wt% Pt leads to an increase in the photocatalytic activity by several times [7]. Another facile technique to increase the activity of TiO_2 is its thermal treatment [8, 9]. According to the literature [9], the annealing of titania may increase the rate of decomposition of methylene blue by approximately four times.

Despite the simplicity of the latter approach, the reasons for the observed increase in activity are still under debate. Moreover, conflicting points of view are given in the literature. For example, S. Sugapriya et al. [8] studied the effect of annealing of TiO_2 nanoparticles and found that their photocatalytic performance is improved due to the transformation of amorphous titanium dioxide to anatase at 450 °C. M. Fassier et al. [9] concluded that the crystallite size is the most important controlling factor for photocatalytic activity rather than the powder specific surface area or the anatase/rutile polymorph ratio. In contrast, R. Su et al. [10] found strong influence of the anatase/rutile ratio on the photoreactivity in the oxidation of methylene blue under UV radiation.

Herein we present a new insight into the thermal activation of TiO_2-based photocatalysts. To elucidate the origin of this effect we prepared Pt/TiO_2 photocatalysts using fresh and thermal-activated Evonik Aeroxide P25 TiO_2 and checked their photoreactivity in the hydrogen production. We chose the photocatalytic production of hydrogen from an aqueous solution of glycerol as a case photocatalytic reaction due to its practical importance. Indeed, glycerol is one of biomass-derived materials, and it is produced in large amounts as a by-product in the transesterification of vegetable oils into biodiesel fuels [4]. Besides, photoreforming of glycerol can provide the yield of seven moles of hydrogen from one mole of glycerol under mild conditions that is made this process suitable for industrial applications.

2 Experimental

2.1 Materials

To prepare the photocatalysts, we used commercial Evonik Aeroxide P25 (formerly known as Degussa P25) titanium dioxide synthesized via flame pyrolysis of $TiCl_4$. Fresh Aeroxide consists of multiphase TiO_2 nanoparticles containing anatase, rutile, and a small amount of amorphous TiO_2 [11]. The thermal activation of titania was performed by calcination in air at 300, 400, 500, 600, 700, or 800 °C in a programmable electric furnace. This heat treatment was performed for approximately 5 h; the thermal profile included the slow heating from room temperature to the desired temperature during 1 h with a constant heating rate, the temperature holding with an accuracy of 10 °C for 3 h, and the spontaneous cooling after turning off the furnace. The Pt/TiO_2 photocatalysts were prepared by impregnation of fresh or calcinated titania with an aqueous solution of H_2PtCl_6 (Reakhim, Russia, 98%) followed by reduction in an aqueous solution of

$NaBH_4$ (Acros Organics, 98%) at room temperature [7]. The photocatalysts were referred to as "T300", "T400", "T500", "T600", "T700", and "T800", respectively. The photocatalyst prepared without the thermal activation was referred to as "RT". Platinum content was approximately 1 wt% in all the photocatalysts. All the chemical reagents used in the experiments, excluding distilled water, were obtained from commercial sources as guaranteed-grade reagents and were used without further purification and treatment.

2.2 Methods

The photocatalysts were examined by UV-vis spectroscopy, X-ray photoelectron spectroscopy (XPS), X-ray absorption near edge structure (XANES) spectroscopy, and X-ray diffraction (XRD) and N_2 adsorption techniques. The diffuse reflectance UV-vis spectra were obtained using a Shimadzu UV-2501 PC spectrophotometer with an ISR-240A diffuse reflectance unit. The specific surface area (SSA) was calculated by the Brunauer–Emmett–Teller method using nitrogen adsorption isotherms measured at liquid nitrogen temperatures with an automatic Micromeritics ASAP 2400 sorptometer. XRD patterns were recorded on a Bruker D8 Advance diffractometer in the 2θ range from 20° to 80° using the Cu *Kα* radiation. The mean sizes of crystallites in the samples were estimated from the full width at half maximum of corresponding peaks using the Scherrer formula. The phase composition of the photocatalysts was quantitatively analyzed using the Rietveld refinement method.

The XPS study was performed using an X-ray photoelectron spectrometer (SPECS Surface Nano Analysis GmbH, Germany) equipped with a PHOIBOS-150 hemispherical electron energy analyzer, a XR-50M X-ray source, and an ellipsoidal crystal monochromator FOCUS-500. The core-level spectra were obtained under ultrahigh vacuum conditions using the monochromatic Al *Kα* radiation. The charge correction was performed by setting the Ti$2p_{3/2}$ peak at 459.0 eV [12]. In this case, the main peak in the C*1s* spectra was observed at 285.2±0.1 eV. Relative concentrations of elements were determined from the integral intensities of the core-level spectra using the cross sections according to Scofield [13]. For detailed analysis, the spectra were fitted into several peaks after the background subtraction by the Shirley method. The fitting procedure was performed using the CasaXPS software. The line shapes of the peaks were approximated by the multiplication of Gaussian and Lorentzian functions.

The Ti K-edge XANES spectra of the Pt/TiO_2 photocatalysts and reference anatase and rutile samples were obtained at the P65 beamline at the synchrotron radiation facility PETRA III (DESY, Hamburg) [14]. A double-crystal fixed-exit monochromator based on Si(111) single-crystals designed by Oxford Ltd. was used. The monochromator was cooled to liquid nitrogen temperature in order to reduce lattice strain by the heat-load impinging on the first crystal. XANES spectra were

measured in the fluorescence detection mode using a passivated implanted planar silicon (PIPS) detector. The XANES spectra were analyzed with the Demeter (IFEFFIT) program package [15].

The photocatalytic activity of the Pt/TiO_2 catalysts was measured for the hydrogen production from a mixture of glycerol and water in a laboratory-made batch reactor. The experiments were performed at atmospheric pressure and at room temperature. The volume of the reactor was 125 cm^3. Before the experiment, 50 mg of a photocatalyst was suspended in the solution, which contained 2.8 mL of glycerol, 97.2 mL of water, and 200 mg of NaOH. The reactor was loaded by this suspension and then was purged with Ar for 30 min. After that, the suspension was illuminated using a 30 W LED lamp with a wavelength of 380 nm (the emission spectrum is present in Fig. S1). The procedure for determining the rate of hydrogen production is described in detail in Supporting Information.

3 Results and discussion

Aeroxide is cheap and extremely photoactive in many photocatalytic reactions, and as a result has become almost the "gold standard" in semiconductor photochemistry research [16]. However, bare Aeroxide exhibits a very low activity in photoreforming of glycerol (0.15 μmol H_2 min^{-1} for the uncalcinated sample). The platinum deposition leads to an increase in activity by more than an order of magnitude. The results of photocatalytic tests of the fresh and thermal-activated platinized samples are presented in Fig. 1. One can see that the thermal treatment increases photoreactivity of Pt/TiO_2 in the hydrogen production. An exception is the sample calcined at 800 °C, which exhibits a very low activity. The maximum activity, 3.6 mmol H_2 min^{-1}, or 4.3 mmol g^{-1} h^{-1} is observed for the sample calcined at 500 °C, while the further increase of the calcination temperature leads to a decrease in the photoactivity. The highest quantum efficiency is 1.2% (λ = 380 nm). This value is quite good for the hydrogen production from a glycerol solution (Table S1).

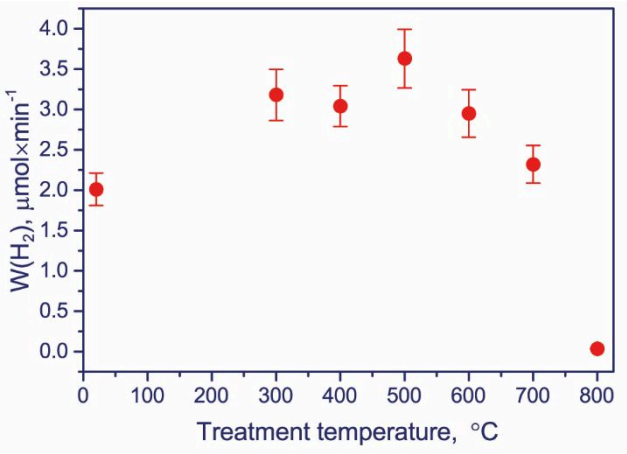

Fig. 1 Photocatalytic production of hydrogen from an aqueous solution of glycerol on Pt/TiO_2 under UV radiation depending on the calcination temperature

To refine the activation effects, morphology, chemistry, and phase composition of the photocatalysts were studied. Table 1 shows the main properties of the fresh and thermal-activated Pt/TiO_2 photocatalysts. All the samples exhibit well developed XRD patterns (Fig. S2), which match well with anatase, rutile, and metallic platinum.

No changes in the structural and textural properties were observed after the calcination at temperatures below 600 °C. According to the Rietveld refinement, the ratio of anatase to rutile (A/R) in the uncalcined photocatalysts and in the Pt/TiO_2 photocatalysts calcined at 300, 400, and 500 °C is 85/15. The mean size of crystallites (D) determined by the Scherrer formula for anatase and platinum is also constant, while the mean size of rutile crystallites increases slightly with the calcination temperature. The specific surface area and the pore volume V are 52-55 m^2/g and 0.43-0.50 cm^3/g, respectively; some deviation observed in these values is due to experimental errors. All these parameters drastically change after the calcination at 700 and 800 °C due to rutile formation. Indeed, it is well known that titanium dioxide, the only naturally occurring oxide of titanium at atmospheric pressure, exhibits three polymorphs: rutile, anatase, and brookite [17]. While rutile is the stable phase, both anatase and brookite are metastable. In the photocatalysts under study, brookite was not detected. At temperature above 600 °C, anatase starts to transform to rutile and after the calcination at 800 °C, no anatase was detected by XRD. This process is accompanied by a strong decrease in the specific surface area and in the pore volume, whereas the mean size of rutile crystallites increases from 32 to 125 nm (Table 1).

Table 1 Properties of fresh and thermal-activated Pt/TiO_2 photocatalysts

Sample	D* of anatase, nm	D* of rutile, nm	D* of Pt, nm	A/R from XRD	A/R from XANES	SSA, m^2/g	V**, cm^3/g	[O]/[Ti] from XPS TiO_2
RT	19	30	4.6	85/15	89/11	55	0.48	2.07
T300	19	30	4.4	85/15	90/10	55	0.50	2.16
T400	19	31	4.6	85/15	86/14	53	0.43	2.26
T500	19	31	4.5	85/15	85/15	52	0.49	2.42
T600	19	32	4.3	84/16	87/13	55	0.52	2.41
T700	29	74	4.4	14/86	22/78	19	0.074	2.69
T800	-	125	5.3	0/100	0/100	10	0.035	2.43

* Crystalline size calculated using the Scherrer equation

** Pore volume determined by low temperature adsorption of N_2

The XRD data are confirmed by UV-vis spectroscopy. The UV-vis diffuse reflectance spectra of the fresh and thermal-activated photocatalysts are presented in Fig. 2. All the spectra contain a single steep absorption edge around 400 nm corresponding to its bandgap. The spectra of the photocatalysts calcined at 700 and 800 °C show a red shift, indicating formation of rutile. Indeed, the optical properties of titanium dioxide depend on its crystal structure. In particular, the optical bandgap of anatase is 3.23 eV (384 nm), whereas that of rutile is 3.02 eV (410 nm) [18].

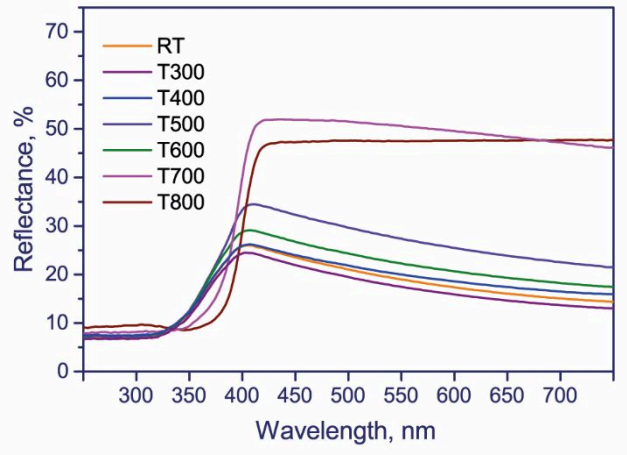

Fig. 2 Diffuse reflectance spectra of fresh and activated Pt/TiO_2 photocatalysts

Hence, our data indicate that the enhanced activity of the Pt/TiO_2 photocatalysts obtained via the thermal activation at 300-500 °C is not a result of changes in its texture properties or the anatase/rutile ratio. However, it is likely that the methods used cannot detect some structural features of the photocatalysts. For instance, R.I. Bickley et al. [19] suggested that some individual anatase nanoparticles may be covered by a thin overlayer of rutile and the photocatalytic activity of this form of titanium dioxide may be greater than the activity of either pure crystalline phase. To check the presence of an excess of rutile, undetectable by XRD, all the photocatalysts were investigated by XANES. It should be stressed that XANES are sensitive not only to the oxidation state of specific atoms but also to its local chemical environment.

The Ti K-edge XANES spectra of the Pt/TiO_2 photocatalysts are presented in Fig. 3a in comparison to the spectra of bulk anatase and bulk rutile. One can see that the spectra of anatase and rutile differ significantly. The spectrum of anatase contains two strong peaks at 4987 and 5003 eV, while the spectrum of rutile contains three strong peaks at 4987, 4992, and 5004 eV. This is in full agreement with the literature [20]. The spectra of the fresh Pt/TiO_2 photocatalyst and the Pt/TiO_2 photocatalysts calcined at 300-500 °C are similar to the spectrum of anatase, whereas the spectra of the Pt/TiO_2 photocatalysts calcined at 700 and 800 °C are similar to the spectrum of rutile.

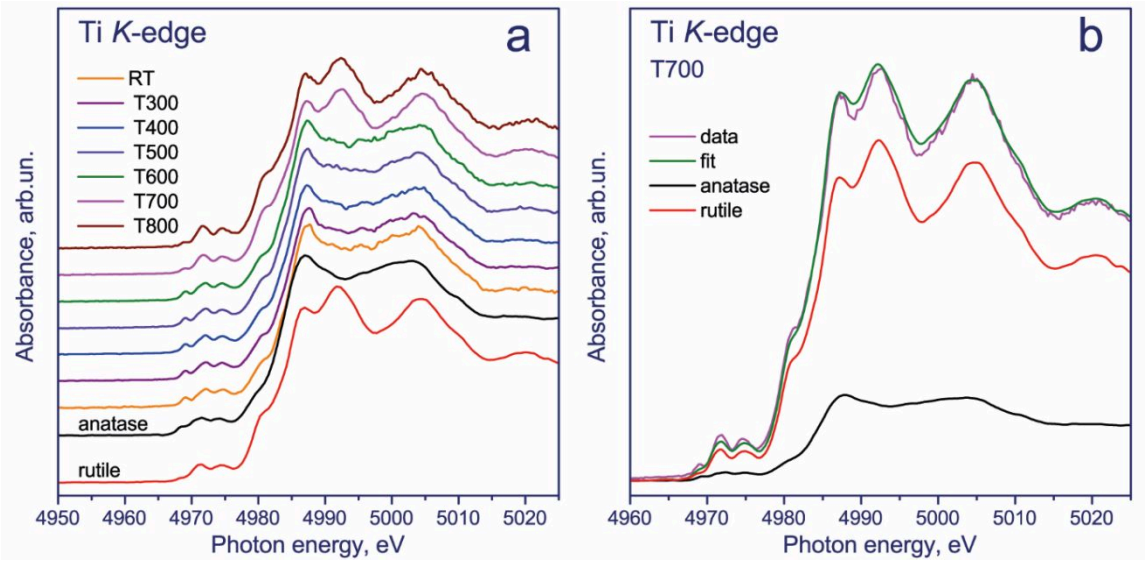

Fig. 3 Normalized Ti K-edge XANES spectra of bulk anatase, bulk rutile, and the fresh and thermally activated Pt/TiO_2 photocatalysts (a); approximation of the XANES spectrum of Pt/TiO_2-T700 by a linear combination of spectra of anatase and rutile (b)

The simplest approach in the XANES data-processing is a linear combination fitting (LCF) [21]. In the LCF method, the X-ray absorption spectrum is modelled by the least-squares fitting using a linear combination of known species to fit an unknown spectrum. In our case, the Ti K-edge XANES spectra of the photocatalysts were well approximated by a linear combination of the spectra of anatase and rutile. The approximation of the XANES spectrum of the T700 photocatalyst by a linear combination of spectra of anatase and rutile is shown in Fig. 3b.

The anatase/rutile ratios determined by the LCF method are presented in Table 1. One can see that XANES gives a higher anatase content in the photocatalysts than XRD does. We can speculate that at least the fresh photocatalyst and the samples calcined at 300 and 400 °C have this effect due to the presence of amorphous TiO_2 whose Ti K-edge XANES spectrum is similar to the spectrum of anatase [20]. The calcination at higher temperatures leads to the transformation of amorphous TiO_2 to anatase and further to rutile. As a result, both XRD and XANES give the same anatase/rutile ratio for the photocatalyst calcined at 500 °C. This finding indicated that the thermal activation at 500 °C leads to remove amorphous TiO_2 which positively affects the activity of the resulting Pt/TiO_2 photocatalyst as it provides a good contact of the platinum nanoparticles and anatase necessary for the formation of the Schottky barrier.

Finally, we investigated the photocatalysts by XPS. The Pt*4f* and Ti*2p* core-level spectra of the fresh and activated Pt/TiO_2 photocatalysts are presented in Figures 4a and 4b. It is known that the ***4f*** level of platinum splits to the Pt$4f_{7/2}$ and Pt$4f_{5/2}$ sublevels due to spin-orbital interaction. The Pt*4f* spectra of all the catalysts were approximated by one asymmetric doublet with the Pt$4f_{7/2}$ binding

energy of 71.1±0.1 eV with the spin-orbital splitting of 3.33 eV (Fig. 4a), which is typical of platinum in the metallic state [22]. For the fresh photocatalyst and the photocatalysts calcined at 300, 400, 500, and 600 °C the [Pt]/[Ti] atomic ratio is in the range 0.015-0.017, which slightly increases with the calcination temperature. The [Pt]/[Ti] atomic ratio for the Pt/TiO_2 photocatalysts calcined at 700 and 800 °C increases to 0.037 and 0.058, respectively This is in good agreement with the XRD data (Table 1), which indicates that the dispersion of the platinum nanoparticles does not change with the calcination temperature with the exception of 800 °C when the mean size of nanoparticles slightly increases because of low surface area of titania. Since XPS is a surface-sensitive method, the increase in the [Pt]/[Ti] atomic ratio for the T700 and T800 photocatalysts is caused by a decrease in the specific surface area.

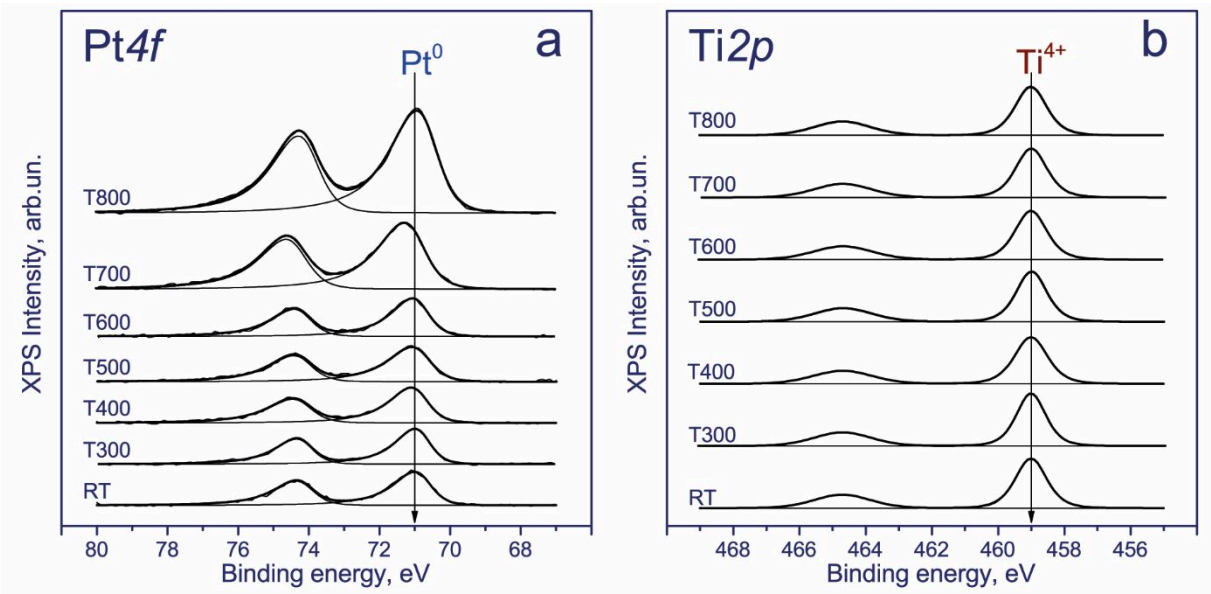

Fig. 4 Normalized Pt*4f* (a) and Ti*2p* (b) core-level spectra of studied catalysts. The Pt*4f* spectra are normalized to the integrated intensity of corresponding Ti*2p* spectra

All the Ti*2p* spectra contain two sharp peaks corresponding to the Ti$2p_{3/2}$ and Ti$2p_{1/2}$ sublevels (Fig. 4b). The peaks have symmetric shape, which is typical of titanium in the oxidized state. Taking into account the Ti$2p_{3/2}$ binding energy of 459.0 eV and the spin-orbital splitting of 5.66 eV, we concluded that titanium is mainly in the Ti^{4+} state. No additional peaks were observed at lower binding energy, which may be attributed to reduced titanium species, such as Ti^{3+}. According to the literature, the Ti$2p_{3/2}$ binding energy for TiO_2 is in the range of 458.7-459.2 eV, whereas for titanium in the Ti^{3+} state, the binding energy is between 456.2 and 457.4 eV [12]. This is an expected result because the thermal activation was performed in air. The formation of Ti^{3+} defects in TiO_2, which is usually accompanied by the formation of oxygen vacancies, was detected after the annealing of anatase in a reducing atmosphere, such as vacuum or hydrogen [23]. At the same time, we found that the calcination of TiO_2 leads to an increase in the [O]/[Ti] atomic ratio (Table 1). The

fresh Pt/TiO_2 photocatalyst is characterized by the [O]/[Ti] atomic ratio equal to 2.07, which is close to the stoichiometric value. This ratio monotonously increases from 2.16 to 2.42 when the calcination temperature increases from 300 to 500 °C. This means that the thermal activation leads to the formation of cationic vacancies.

It should be noted that the formation of cationic vacancies in titania is not a new effect. Recently, Ghosh and Nambissan [24] studied the annealing of anatase nanoparticles. Using photoluminescence spectroscopy, they showed the formation of vacancy-type defects such as oxygen vacancy (V_O), cation vacancy (V_{Ti}) or vacancy-combination defects. The application of positron annihilation spectroscopy and Coincident Doppler broadening spectroscopy made it possible to prove the formation of cation vacancy V_{Ti} and larger vacancy-combination defects as divacancy V_{Ti+O} and trivacancy $V_{Ti+O+Ti}$. During the annealing, the concentration of such defect-combinations initially increases to a maximum at approximately 300 °C and then decreases at higher temperatures due to gradual annealing. We can speculate that the divacancy V_{Ti+O} and trivacancy $V_{Ti+O+Ti}$ are also formed during the thermal activation of our photocatalysts. According to XPS (Table 1) the concentration of cation vacancies in our titania samples increases with the calcination temperature excepting 800 °C when anatase transforms to rutile in full. Being negatively charged, these defects within TiO_2 nanoparticles could play the role of hole traps, thereby increasing the lifetime of electron-hole pairs in the semiconductor and increasing their photoreactivity. Certainly, some additional experiments and DFT calculations should be performed to study in detail the formation of the cationic vacancies in titania and their role in photocatalytic reactions.

4 Conclusions

The Pt/TiO_2 photocatalysts prepared by fresh and thermal-activated Evonik Aeroxide P25 TiO_2 were tested in the production of hydrogen from aqueous solutions of glycerol under UV radiation. It was found that the thermal activation of titania in the temperature range between 300 and 600 °C leads to an increase in the photoreactivity of resulting Pt/TiO_2 photocatalysts. The highest activity was obtained after annealing at 500 °C. According to the XPS study this effect is due to formation of cationic vacancies that limit the fast electron-hole recombination. After annealing at 700-800 °C, anatase transforms irreversibly to rutile which typically has less photoreactivity due to shorter lifetime of electron-hole pairs. Moreover, the rutile formation is accompanied by a strong decrease in the specific surface area, which also negatively affects the rate of hydrogen production. Hence, the thermal activation of titania at 500 °C can be used to improve the activity of titania-based photocatalysts. In addition it was found that the thermal activation at 500 °C leads to remove amorphous TiO_2 which positively affects the activity of the resulting Pt/TiO_2 photocatalyst as it

provides a good contact of the platinum nanoparticles and anatase necessary for the formation of the Schottky barrier. Hence, both these effects, the creation of cationic vacancies and transformation of amorphous TiO_2 to anatase under the thermal activation can provide enhanced photocatalytic activity of Pt/TiO_2 photocatalysts.

Acknowledgments This work was supported by Russian Science Foundation (grant #19-73-20020). The XPS and XRD experiments were performed using facilities of the shared research center "National center of investigation of catalysts" at Boreskov Institute of Catalysis. The authors are grateful to S. Cherepanova for the XRD study and T. Larina for the UV-vis measurements. The authors are also grateful to the staff of DESY for their support during the beam time.

Compliance with Ethical Standards

Conflict of interest The authors declare that they have no conflict of interest.

Electronic supplementary material The online version of this article (https://doi.org/) contains supplementary material, which is available to authorized users.

References

1. Fujishima A, Honda K (1972) Electrochemical photolysis of water at a semiconductor electrode. Nature 238:37–38. https://doi.org/10.1038/238037a0
2. Kozlova EA, Markovskaya DV, Cherepanova SV, Saraev AA, Gerasimov EY. Perevalov TV, Kaichev VV, Parmon VN (2014) Novel photocatalysts based on $Cd_{1-x}Zn_xS/Zn(OH)_2$ for the hydrogen evolution from water solutions of ethanol. Int. J. Hydrogen Energy 39:18758–18769. https://doi.org/10.1016/j.ijhydene.2014.08.145
3. Kozlova EA, Parmon VN (2017) Heterogeneous semiconductor photocatalysts for hydrogen production from aqueous solutions of electron donors. Russ Chem Rev 86:870–906. https://doi.org/10.1070/RCR4739
4. Fujita SI, Kawamori H, Honda D, Yoshida H, Arai M (2016) Photocatalytic hydrogen production from aqueous glycerol solution using NiO/TiO_2 catalysts: Effects of preparation and reaction conditions. Appl Catal B 181:818–824. https://doi.org/10.1016/j.apcatb.2015.08.048
5. Schneider J, Matsuoka M, Takeuchi M, Zhang J, Horiuchi Y (2014) Understanding TiO_2 photocatalysis: Mechanisms and materials. Chem Rev 114:9919–9986. https://doi.org/10.1021/cr5001892
6. Linsebigler AL, Lu G, Yates JT, Jr (1995) Photocatalysis on TiO_2 surfaces: Principles, mechanisms, and selected results. Chem Rev 95:735–758. https://doi.org/10.1021/cr00035a013

7. Kozlova EA, Lyubina TP, Nasalevich MA, Vorontsov AV, Miller AV, Kaichev VV, Parmon VN (2011) Influence of the method of platinum deposition on activity and stability of Pt/TiO_2 photocatalysts in the photocatalytic oxidation of dimethyl methylphosphonate. Catal Commun 12:597–601. https://doi.org/10.1016/j.catcom.2010.12.007
8. Sugapriya S, Sriram R, Lakshmi S (2013) Effect of annealing on TiO_2 nanoparticles. Optik 124:4971–4975. https://doi.org/10.1016/j.ijleo.2013.03.040
9. Fassier M, Peyratout CS, Smith DS, Ducroquetz C, Voland T (2010) Photocatalytic activity of titanium dioxide coatings: Influence of the firing temperature of the chemical gel. J Eur Ceram Soc 30:2757–2762. https://doi.org/10.1016/j.jeurceramsoc.2010.05.018
10. Su R, Bechstein R, Sø L, Vang RT, Sillassen M, Esbjörnsson B, Palmqvist A, Besenbacher F (2011) How the anatase-to-rutile ratio influences the photoreactivity of TiO_2. J Phys Chem C 115:24287–24292. https://doi.org/10.1021/jp2086768
11. Jiang X, Manawan M, Feng T, Qian R, Zhao T, Zhou G, Kong F, Wang Q, Dai S, Pan JH (2018) Anatase and rutile in evonik aeroxide P25: Heterojunctioned or individual nanoparticles? Catal Today 300:12–17. https://doi.org/10.1016/j.cattod.2017.06.010
12. Kaichev VV, Popova GY, Chesalov YA, Saraev AA, Zemlyanov DY, Beloshapkin SA, Knop-Gericke A, Schlögl R, Andrushkevich TV, Bukhtiyarov VI (2014) Selective oxidation of methanol to form dimethoxymethane and methyl formate over a monolayer V_2O_5/TiO_2 catalyst. J Catal 311:59–70. http://doi.org/10.1016/j.jcat.2013.10.026
13. Scofield JH (1976) Hartree-Slater subshell photoionization cross-sections at 1254 and 1487 eV. J Electron Spectrosc Relat Phenom 8:129–137. https://doi.org/10.1016/0368-2048(76)80015-1
14. Caliebe WA, Murzin V, Kalinko A, Görlitz M (2019) High-flux XAFS-beamline P64 at PETRA III. AIP Conf Proc 2054:060031. https://doi.org/10.1063/1.5084662
15. Ravel B, Newville M (2005) ATHENA, ARTEMIS, HEPHAESTUS: data analysis for X-ray absorption spectroscopy using IFEFFIT. J Synchrotron Rad 12:537–541. https://doi.org/10.1107/S0909049505012719
16. Mills A, Lee SK (2002) A web-based overview of semiconductor photochemistry-based current commercial applications. J Photochem Photobiology A 152:233–247. https://doi.org/10.1016/S1010-6030(02)00243-5
17. Hanaor DAH, Sorrell CC (2011) Review of the anatase to rutile phase transformation. J Mater Sci 46:855–874. https://doi.org/10.1007/s10853-010-5113-0
18. Mills A, Lee SK (2003) Platinum group metals and their oxides in semiconductor photosensitization. Platinum Metals Rev 47:2–12. https://www.technology.matthey.com/article/47/1/2-12/

19. Bickley RI, Gonzalez-Carreno T, Lees JS, Palmisano L, Tilley RJD (1991) A structural investigation of titanium dioxide photocatalysts. J Solid State Chem 92:178–190. http://dx.doi.org/10.1016/0022-4596(91)90255-G
20. Zhang H, Chen B, Banfield JF (2008) Atomic structure of nanometer-sized amorphous TiO_2. Phys Rev B 78:214106. https://doi.org/10.1103/PhysRevB.78.214106
21. Fedorov AV, Tsapina AM, Bulavchenko OA, Saraev AA, Odegova GV, Ermakov DY, Zubavichus YV, Yakovlev VA, Kaichev VV (2018) Structure and chemistry of Cu–Fe–Al nanocomposite catalysts for CO oxidation. Catal Lett 148:3715–3722. https://doi.org/10.1007/s10562-018-2539-5
22. Miller AV, Kaichev VV, Prosvirin IP, Bukhtiyarov VI (2013) Mechanistic study of methanol decomposition and oxidation on Pt(111). J Phys Chem C 117:8189–8197. https://doi.org/10.1021/jp3122177
23. Xiong LB, Li JL, Yang B, Yu Y (2011) Ti^{3+} in the surface of titanium dioxide: Generation, properties and photocatalytic application. J Nanomater 2012:831524. https://doi.org/10.1155/2012/831524
24. Ghosh S, Nambissan PMG (2019) Evidence of oxygen and Ti vacancy induced ferromagnetism in post-annealed undoped anatase TiO_2 nanocrystals: A spectroscopic analysis. J Solid State Chem 275:174–180. https://doi.org/10.1016/j.jssc.2019.04.010